Sensitivity of coherent dual-comb spectroscopy

Nathan R. Newbury,* Ian Coddington, and William Swann

National Institute of Standards and Technology, 325 Broadway, Boulder, CO 80305 USA
*nnewbury@boulder.nist.gov

Abstract: Coherent dual comb spectroscopy can provide high-resolution, high-accuracy measurements of a sample response in both magnitude and phase. We discuss the achievable signal-to-noise ratio (SNR) due to both additive white noise and multiplicative noise, and the corresponding sensitivity limit for trace gas detection. We show that sequential acquisition of the overall spectrum through a tunable filter, or parallel acquisition of the overall spectrum through a detector array, can significantly improve the SNR under some circumstances. We identify a useful figure of merit as the quality factor, equal to the product of the SNR, normalized by the square root of the acquisition time, and the number of resolved frequency elements. For a single detector and fiber-laser based system, this quality factor is 10^6 - 10^7 $Hz^{1/2}$.

OCIS codes: (300.6320) Spectroscopy, heterodyne; (300.6300) Spectroscopy, Fourier transforms

References and links

1. F. Keilmann, C. Gohle, and R. Holzwarth, "Time-domain mid-infrared frequency-comb spectrometer", Opt. Lett. **29**, 1542–1544 (2004).
2. A. Schliesser, M. Brehm, F. Keilmann, and D. van der Weide, "Frequency-comb infrared spectrometer for rapid, remote chemical sensing", Opt. Express **13**, 9029–9038 (2005).
3. T. Yasui, Y. Kabetani, E. Saneyoshi, S. Yokoyama, and T. Araki, "Terahertz frequency comb by multifrequency-heterodyning photoconductive detection for high-accuracy, high-resolution terahertz spectroscopy", Appl. Phys. Lett. **88**, 241104 (2006).
4. P. Giaccari, J. D. Deschenes, P. Saucier, J. Genest, and P. Tremblay, "Active fourier-transform spectroscopy combining the direct rf beating of two fiber-based mode-locked lasers with a novel referencing method", Opt. Express **16**, 4347–4365 (2008).
5. B. Bernhardt, A. Ozawa, P. Jacquet, M. Jacquey, Y. Kobayashi, T. Udem, R. Holzwarth, G. Guelachvili, T. W. Hansch, and N. Picque, "Cavity-enhanced dual-comb spectroscopy", Nat. Photon. **4**, 55–57 (2009).
6. I. Coddington, W. C. Swann, and N. R. Newbury, "Coherent multiheterodyne spectroscopy using stabilized optical frequency combs", Phys. Rev. Lett. **100**, 013902 (2008).
7. I. Coddington, W. Swann, and N. Newbury, "Time-domain spectroscopy of molecular free-induction decay in the infrared", Opt. Lett., accepted (2010).
8. I. Coddington, W. Swann, and N. Newbury, "Coherent dual-comb spectroscopy at high signal to noise", http://arxiv.org/abs/1001.3865 (2010).
9. R. J. Bell, *Introductory Fourier transform spectroscopy* (Academic Press, 1972).
10. J. Chamberlain, *The Principles of Interferometric Spectroscopy* (John Wiley and Sons, Inc, 1979).
11. J. R. Birch, "Dispersive fourier-transform spectroscopy", Mikrochimica Acta **3**, 105–122 (1987).
12. N. Almoayed and M. Afsar, "High-resolution absorption coefficient and refractive index spectra of carbon monoxide gas at millimeter and submillimeter wave-lengths", IEEE T. Instrum. Meas. **55**, 1033–1037 (2006).
13. S. Schiller, "Spectrometry with frequency combs", Opt. Lett. **27**, 766–768 (2002).
14. J. W. Brault, *High Resolution in Astronomy* (Geneva Observatory, 1985), Fourier transform spectrometry, pp. 1–65.
15. L. A. Sromovsky, "Radiometric errors in complex fourier transform spectrometry", Appl. Opt. **42**, 1779–1787 (2003).
16. S. P. Davis, M. C. Abrams, and J. W. Brault, *Fourier Transform Spectrometry* (Academic Press, 2001).
17. V. V. Protopopov, *Laser Heterodyning* (Springer Berlin / Heidelberg, 2009).
18. W. Demtroder, *Laser Spectroscopy* (Springer, 1996), 2nd ed.
19. I. Coddington, W. C. Swann, and N. R. Newbury, "Coherent linear optical sampling at 15 bits of resolution", Opt. Lett. **34**, 2153–2155 (2009).

#123518 - $15.00 USD Received 29 Jan 2010; revised 12 Mar 2010; accepted 15 Mar 2010; published 31 Mar 2010

20. N. R. Newbury and W. C. Swann, "Low-noise fiber-laser frequency combs (invited)", J. Opt. Soc. Am. B **24**, 1756–1770 (2007).
21. J. M. Dudley, G. Genty, and S. Coen, "Supercontinuum generation in photonic crystal fiber", Rev. Mod. Phys. **78**, 1135–1184 (2006).
22. N. R. Newbury, B. R. Washburn, K. L. Corwin, and R. S. Windeler, "Noise amplification during supercontinuum generation in microstructure fiber", Opt. Lett. **28**, 944–946 (2002).
23. K. L. Corwin, N. R. Newbury, J. M. Dudley, S. Coen, S. A. Diddams, K. Weber, and R. S. Windeler, "Fundamental noise limitations to supercontinuum generation in microstructure fiber", Phys. Rev. Lett. **90**, 113904 (2003).
24. T. W. Hänsch, "Nobel lecture: Passion for precision", Rev. Mod. Phys. **78**, 1297–1309 (2006).
25. J. L. Hall, "Nobel lecture: Defining and measuring optical frequencies", Rev. Mod. Phys. **78**, 1279–1295 (2006).

1. Introduction

There have been a number of demonstrations of coherent dual comb spectroscopy [1-8] providing broadband spectroscopic data often with very high frequency accuracy and resolution. In the configuration considered here, and demonstrated fully in Ref. [6-8], the output of one comb is transmitted through a sample and then combined with a second "local oscillator" (LO) comb source to measure the full complex response of a sample (i.e., phase and amplitude) with the frequency resolution and accuracy inherent to the comb source. In the time domain, the approach mirrors time-domain spectroscopy [7] or dispersive Fourier transform spectroscopy (FTS) [9-12]. In the frequency domain, the approach resembles a massively parallel laser heterodyne spectrometer, where each pair of comb teeth contributes to the heterodyne signal at a specific rf frequency [13]. Although this technique can provide the complex response (phase and amplitude) with high frequency accuracy and resolution, the achievable signal-to-noise ratio (SNR) is limited by the usual factors, namely detector noise, shot-noise, technical laser noise and detection dynamic range. A low SNR can, of course, diminish many of the benefits of the approach. For example, the ability to find the line center of broad spectral lines will have a statistical limit set by the SNR that can exceed the inherent comb accuracy. Here we derive scaling laws and quantitative SNR expressions and examine the sensitivity of this technique. These expressions will be useful in system design, in evaluating the system performance, and in comparisons to more conventional approaches.

We derive three main equations. First, we give the limiting SNR due to detector noise, shot noise, excess laser relative intensity noise (RIN), and detector dynamic range. We point out the potential advantages of sequential or parallel acquisition across the full spectrum. We also compare with a tunable laser spectrometer. Second, we give the corresponding sensitivity limit for trace gas detection. Third, we give the SNR limitations due to multiplicative noise, in particular due to residual carrier phase noise between the combs. Under the appropriate operating parameters and with either active phase-locking [6-8] or active monitoring [4] to cancel relative phase and timing jitter between the combs, this multiplicative noise is shown to be negligible. The derivations are straightforward and the final scaling laws follow closely related expressions in conventional FTS [14-16] and laser spectroscopy [17, 18]. Therefore, in Section 2, we present and discuss the basic results and only later in Section 3 do we give a detailed derivation.

2. Sensitivity of dual-comb spectrometers

2.1 Configuration of dual-comb spectrometer

Coherent dual comb spectroscopy can be viewed as a massively parallel multi-heterodyne measurement between a source comb that passes through a sample and an LO comb with a different repetition rate; each pair of comb teeth from the source and LO combs forms its own RF beat signal, thereby down-converting the optical response to the rf domain. In the time domain, the method is essentially Fourier spectroscopy and involves the acquisition of an interferogram (or cross correlation) between the individual pulses of the source, $E_s(t)$, and the LO, $E_{LO}(t)$; the overlap between successive pairs of pulses occurs with an effective time step equal to the difference in pulse periods so that the LO pulses slowly walk through the signal

#123518 - $15.00 USD Received 29 Jan 2010; revised 12 Mar 2010; accepted 15 Mar 2010; published 31 Mar 2010

pulses. In this picture, the digitized voltage with no sample present is $V_{ref}(t) = S(t) \otimes E_s(t)$ as a function of effective time t where $\otimes$ denotes a convolution and $S(t) \sim E_{LO}^{*}(-t)$ is the sampling function. (A more accurate expression for $S(t)$ that preserves the multi-heterodyne frequency-domain picture is given in Eq. (12) and Ref. [19].) In the presence of a sample with time-domain response $H(t)$, the digitized voltage is $V(t) = S(t) \otimes E_s(t) \otimes H(t)$. The goal is to isolate the sample response, which is easily done in the frequency domain from the ratio

$$\tilde{H}(\nu) = \frac{\tilde{V}(\nu)}{\tilde{V}_{ref}(\nu)} = \tilde{H}_0(\nu) + \sigma_H \tag{1}$$

where the tilde represents a Fourier transform and ν is the optical frequency. $\tilde{H}_0(\nu)$ is the true sample response and σ_H is the inevitable added noise, which is the subject of the remainder of this paper. For a weakly absorbing sample, $\tilde{H}_0(\nu) \equiv 1 + 4\pi^2 i c^{-1} \nu \chi(\nu) L \approx 1 - \alpha(\nu) L/2 + i\Delta k(\nu) L$, where χ is the linear susceptibility, L is the sample length, $\alpha(\nu)$ is the attenuation coefficient and $\Delta k(\nu)$ the phase shift.

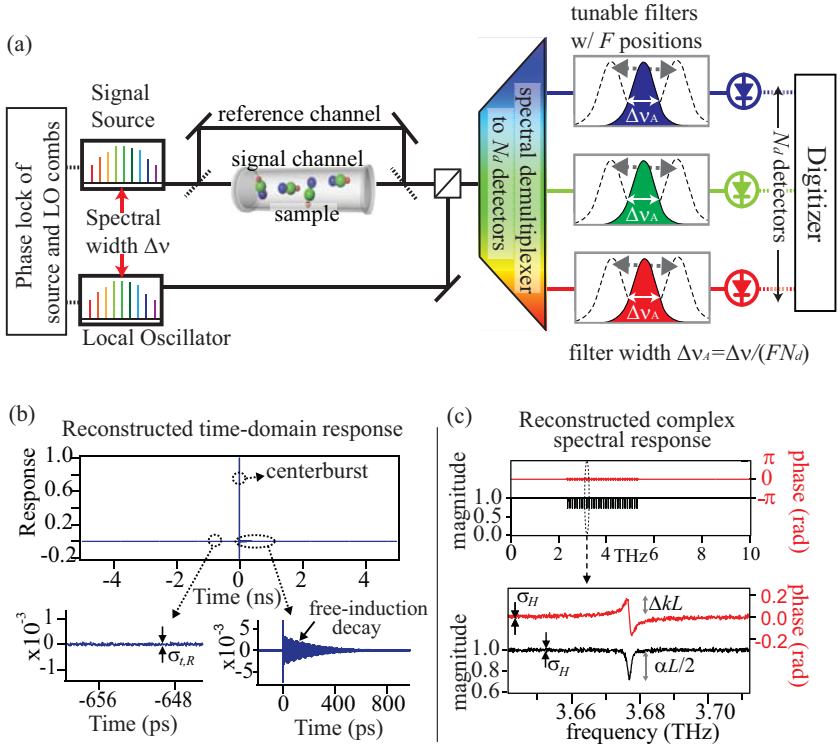

Fig. 1. (a) Schematic of dual-comb layout including the possibility of sequential or parallel data acquisition. In the figure, the signal and reference are time-multiplexed [7, 8], but the reference could also be acquired in a separate interferometer [6] or sequentially with an empty cell. (b) Simulated time-domain signal versus the effective down-converted time (and not laboratory time). (c) Corresponding frequency-domain sample response over a 10 THz window at 100 MHz resolution for $M = 100{,}000$ resolved elements. For illustrative purposes, we assume a sample with 20 equally spaced, Lorentzian transitions 2 GHz wide and a spectral domain SNR of $\sigma_H^{-1} = 100$. In the time domain, the corresponding signal is a one-sided interferogram with two components: a centerburst and a trailing free induction decay signal. In the frequency domain, each transition is highly resolved in magnitude and phase.

#123518 - $15.00 USD Received 29 Jan 2010; revised 12 Mar 2010; accepted 15 Mar 2010; published 31 Mar 2010

We consider the general configuration shown in Fig. 1, which is motivated by the following consideration. While Fourier spectroscopy can significantly reduce the effects of detector noise (Felgett's advantage), it magnifies the effects of excess source noise and dynamic range limitations [9, 10, 14, 16]. These noise terms are mitigated by breaking up the measured spectrum ($\Delta\nu$) into sub-bands that can be acquired sequentially or in parallel. Parallel acquisition is accomplished through a fixed filter that multiplexes N_d spectrally filtered bands to an array of N_d detectors. Sequential acquisition is accomplished through a tunable optical bandpass filter in front of each detector that steps through F different filter bands. In all, the total spectral bandwidth is divided into $F \times N_d$ sub-bands with filtered bandwidth $\Delta\nu_A = \Delta\nu / (FN_d)$. Each sub-band is measured for a period T/F, where T is the total acquisition period. Within each sub-band, the response is calculated according to Eq. (1). The stability of the combs allows one to coherently stitch together the full bandwidth signature from these sub-bands while preserving the frequency resolution and accuracy. In addition to potentially improving the SNR, this spectral division allows for a larger difference in comb repetition rates, Δf_r, (while still satisfying Nyquist constraints). Since this difference, Δf_r, is exactly the separation between the down-converted rf heterodyne beat signals, a larger value of Δf_r translates to a relaxed requirement on the relative comb linewidths. Filtering also helps normalize strong spectral variations in the comb spectra [8]. However, these benefits must be balanced with the fact that spectral division also magnifies multiplicative noise (Section 2.4) and can come with added overhead in time.

We make several assumptions in the analysis. First, we assume negligible differential chirp between the filtered source and LO pulses. Differential chirp between the pulses has the benefit of reducing the dynamic range limitation [4, 16] and furthermore would be cancelled in Eq. (1). However, it can also introduce correlations in the phase and timing noise which are not treated here. Second, we assume the optical filter is Gaussian in shape and calculate the average SNR (equal to σ_H^{-1}) across the central FWHM. Effectively, then, for no filtering ($FN_d = 1$), we assume a Gaussian source spectrum while for filtering ($FN_d > 1$), we assume a roughly uniform source spectrum. Third, we assume the detection is followed by a hardware or software low-pass filter with bandwidth equal to the Nyquist frequency of $f_r/2$. Fourth, we assume that the difference in comb repetition rates, Δf_r, and spectral width of the sub-bands are chosen to satisfy the Nyquist constraint [1-8]. Fifth, we assume that the relative linewidth of the two comb sources is sufficiently controlled to be below Δf_r (i.e. we assume negligible "1/f" noise in relative phase and timing jitter between the combs [20]).

2.2 Effects of additive noise: detector noise, shot noise, laser RIN & detector dynamic range

In terms of noise, we consider detector noise, shot noise, and excess Relative Intensity Noise (RIN). The detector noise is characterized by an effective Noise Equivalent Power (NEP) that includes any and all additive noise terms up to the digitization of the signal such as dark current, Johnson noise, amplifier noise figure etc. This NEP will vary significantly depending on wavelength band and type of detector. We do assume the heterodyne signal is at high enough frequency to be well away from any "1/f" detection so that the NEP is white with frequency. The shot noise is easily calculated from the comb power, evaluated at the photodetector. The laser RIN can have a component at lower frequencies from pulse-to-pulse variations and a component at all frequencies from additive amplified spontaneous emission (ASE) emitted from the laser or from any subsequent optical amplification. The low-frequency component can lead to multiplicative noise but we ignore it under the assumption that the interferogram update rate, equal to Δf_r, is faster than this low frequency noise. Alternatively, this RIN component could be experimentally suppressed through active feedback or cancelled through a separate measurement. Therefore, we only consider the white, broadband RIN due to additive ASE. Furthermore, we assume the ASE has the same uniform spectral shape as the comb output. Finally, we also include a dynamic range limit to the detection set by the digitizer, amplifier, or, ultimately, the photodetector itself.

#123518 - $15.00 USD Received 29 Jan 2010; revised 12 Mar 2010; accepted 15 Mar 2010; published 31 Mar 2010

By considering only the white, broadband noise sources above, we essentially assume "perfect" source and LO combs, other than the effect of additive ASE. However, there will also be residual timing and carrier phase noise between the combs that can lead to multiplicative noise. In Section 2.4 and 3.4, we consider the multiplicative noise from carrier phase jitter since it will likely dominate over timing jitter. We show there that the multiplicative noise is negligible provided the optical filter bandwidth is sufficiently large and that the phase jitter is sufficiently suppressed through either active feedback or monitoring.

The measurement of $\tilde{H}(\nu)$ of Eq. (1) yields a set of complex points covering a bandwidth $\Delta\nu$ with M resolved spectral elements. Including only the broadband noise contributions, the averaged uncertainty across the spectrum at each spectral element for the magnitude or phase (in radians) is,

$$\sigma_H = \frac{M\sqrt{\varepsilon}}{0.8\sqrt{T}}\left\{a_{NEP}\frac{F}{P_c^2} + a_{shot}\frac{1}{N_d P_c} + \left(a_{RIN} + a_{range}\right)\frac{1}{N_d^2 F}\right\}^{1/2}, \qquad (2)$$

with the variables given in Table 1. (Eq. (2) is derived in Section 3.2.) The SNR is simply $1/\sigma_H$. The first two terms in the sum are detector noise and shot noise. The last term reflects the limits to measuring a pulse set by either the laser RIN or by detection dynamic range. ε accounts for the mismatch between the required resolution and the resolution set by the comb repetition rate. It can be viewed as a duty cycle correction in the time domain. It is theoretically absent in FTS because the scan length would be matched to the desired resolution (although even then, conventional FTS would still have a similar term due to the turn-around time of the mirror.) Note that modulation of the difference in repetition frequencies [2] can in principle reduce this duty cycle factor.

Table 1. Definition of variables

Quantity (Units)	Variable	Quantity (Units)	Variable
Source comb power (W)	P_c	Spectral width (Hz)	$\Delta\nu$
Source to LO power ratio[a]	γ	Comb repetition rate (Hz)[b]	f_r
LO comb power (W)	γP_c	Spectral resolution (Hz)	ν_{res}
Detector noise (W/Hz$^{1/2}$)	NEP	# of resolution elements	$M = \Delta\nu/\nu_{res}$
Detection dynamic range[c]	D	Duty cycle	$\varepsilon \equiv \nu_{res}/f_r$
Laser Relative Intensity Noise[d]	RIN	# of filters positions (degree of sequential acquisition)	F
Detector efficiency	η	# of detectors (degree of parallel acquisition)	N_d
Balanced detection factor[e]	b		
Coefficients			
$a_{NEP} = \gamma^{-1} NEP^2$	$a_{shot} = 4c_\gamma \eta^{-1} h\nu$	$a_{RIN} = 2c_{\gamma^2} bRIN$	$a_{range} = 8D^{-2} f_r^{-1}$

[a] The related constants are $c_\gamma = (1+\gamma)/(2\gamma)$ and $c_{\gamma 2} = (1+\gamma^2)/(2\gamma)$. γ is closely related to the modulation efficiency in conventional FTS.
[b] Specifically, the source or LO repetition rate is f_{rS} or f_{rL}.
[c] The dynamic range can be related to an effective number of bits N, as $D = \sqrt{3}\, 2^N$ [16]. For $N = 12$, $D \sim 7000$.
[d] The RIN is single-sided. It is typically quoted in dBc/Hz.
[e] Detection can employ balanced detection, for which $b = 1$, or unbalanced detection for which $b = 2$.

#123518 - $15.00 USD Received 29 Jan 2010; revised 12 Mar 2010; accepted 15 Mar 2010; published 31 Mar 2010

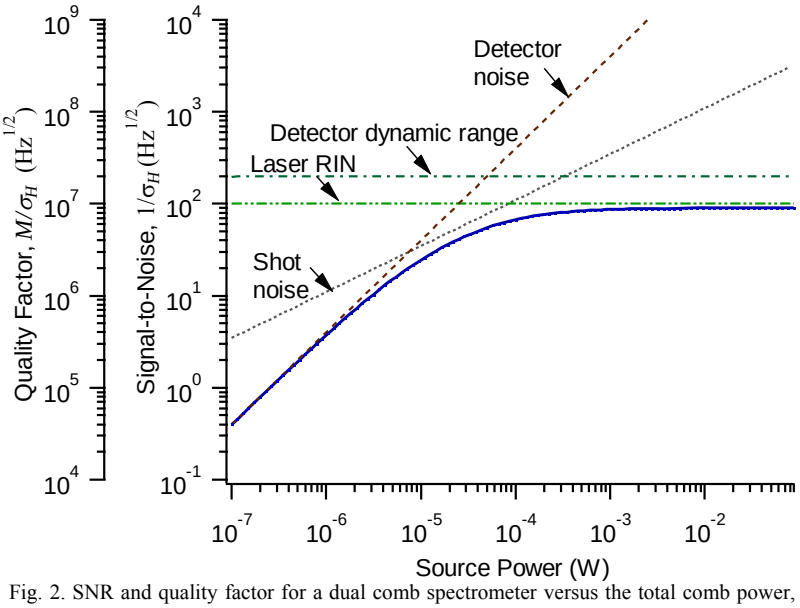

Fig. 2. SNR and quality factor for a dual comb spectrometer versus the total comb power, P_c, for a single detector with no optical filtering ($F = N_d = 1$) from Eq. (2), normalized to a 1 sec total acquisition time. The quality factor is the product of the number of resolved spectral elements and the SNR for either amplitude or phase. The SNR for $M = 100{,}000$ resolved elements is also shown. The SNR (or quality factor) (solid blue line) is limited by detector noise (long dashed brown line) at low comb powers, by shot noise (short dashed grey line) at medium comb powers, and by either laser RIN (dash-dot light green line) or detector dynamic range (dash-dotted dark green line) at high comb powers. With our assumption of a uniform spectrum and Gaussian filter shape, the average power per comb tooth is $P_{tooth} = 0.8 P_c f_r / \Delta\nu$. Values used: NEP = 2 pW/Hz$^{1/2}$, D = 7000, RIN = -145 dBc/Hz, η = 0.9, b = 1, ε=1, $\gamma = c_\gamma = c_{\gamma 2}$=1, $\Delta\nu$ = 10 THz, $f_r = \nu_{res}$ = 100 MHz.

From Eq. (2) regardless of the dominant noise, the uncertainty scales linearly with M. An $M^{1/2}$ dependence is expected in Fourier spectroscopy because there are ~M time steps per interferogram. In dual-comb spectroscopy, an additional $M^{1/2}$ arises because we assume a constant laser power, therefore doubling the spectral width reduces the source spectral power density. In conventional FTS it is not normally present since the source power spectral density is fixed. From both this scaling, and from a practical point of view, a useful figure of merit is the normalized quality factor, M/σ_H at T =1 s [9], or the product of the SNR per unit time and number of resolved spectral elements. Figure 2 plots the quality factor and SNR versus total comb power. In the next subsections, we discuss other consequences of Eq. (2).

2.2.1 Scaling with filtering and number of detectors

Figure 3 illustrates the scaling of the quality factor and SNR with the degree of sequential or parallel spectral acquisition, as quantified by F and N_d. The quantities are all normalized to the same 1 sec total acquisition time. In the detector noise limit (low P_c), there is a distinct disadvantage to sequential acquisition ($F > 1$), as expected from Fellgett's advantage and no benefit to multiple detectors. In the shot noise limit (medium P_c), the same SNR is reached whether the spectrum is measured sequentially or at once, but there is benefit to multiple detectors. Finally, in either the RIN or dynamic range limit (high P_c), there is an advantage to sequential acquisition and an even stronger advantage to multiple detectors.

Increasing the overall degree of filtering, N_dF, reduces the optical power on a given detector and shifts the limiting noise from RIN or dynamic range to either shot noise or detector noise. Ideally, one would like to increase the number of detectors, N_d, until the noise is limited by the detector noise. In practice, the use of multiple detectors must be balanced by

#123518 - $15.00 USD Received 29 Jan 2010; revised 12 Mar 2010; accepted 15 Mar 2010; published 31 Mar 2010

the corresponding increase in system complexity and for practical reasons N_d may be limited to one. It is still advantageous to then increase the sequential filtering, F, until the RIN or dynamic range no longer dominates. Based on Eq. (2), the optimal value of spectral filtering is $F_{opt} \approx P_c\sqrt{2RIN}\big/\left(N_d NEP\right)$ (for large D and $\varepsilon = b = \gamma = c_{\gamma^2} = 1$). For the values in Fig. 1 and P_c=2 mW, one finds $F_{opt} \approx 100 N_d^{-1}$, corresponding to ~ 1 nm bandwidth filtering for a 10 THz source at 1550 nm. This bandwidth is probably too narrow given the need to suppress the effects of multiplicative noise (see Section 2.5) and one would likely operate the system at a slightly broader filtering level.

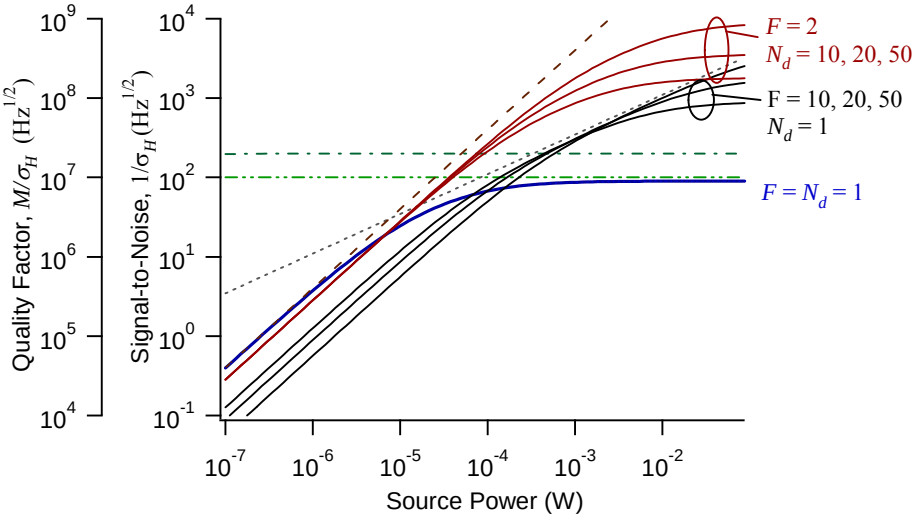

Fig. 3. Quality factor and SNR at M = 100,000 resolved elements versus the total comb power, P_c, for different values of sequential acquisition at F = 10, 20, 50 and N_d = 1 (black lines) and parallel data acquisition at N_d = 10, 20, 50 detectors and F = 2 (red lines) under the otherwise identical conditions to Figure 2. The additional lines are carried over from Figure 2 for reference. The use of sequential acquisition comes at a cost for low powers, but at high comb powers can remove the limitations otherwise imposed by laser RIN or detector dynamic range. The effects of multiplicative noise (see Section 2.4) are not included. (The curves for $N_d > 1$ use F = 2 since an interleaved approach would likely be used.)

2.2.2 Quantitative values and comparison with existing demonstrations

In general, for systems operating near the gain bandwidth of the laser or amplifier, the comb power can be high enough that we expect the limiting noise term in Eq. (2) to be the RIN/dynamic range term, at least for a low F and N_d. For supercontinuum sources, it may well dominate as well due to the degradation in RIN [21-23]. In this limit, Eq. (2) can be rewritten as the quality factor in the simplified expression,

$$\frac{M}{\sigma_H} = 0.8\frac{N_d\sqrt{T}}{\sqrt{\varepsilon}}\sqrt{\frac{F}{2RIN + 8D^{-2}f_r^{-1}}} \tag{3}$$

for $b = \gamma = c_{\gamma^2} = 1$. We measure fiber-laser RINs as low as 10^{-15}, or -150 dBc/Hz. However, with amplification, values of -145 dBc/Hz are perhaps more realistic, and even higher RIN may be reached for significant spectral broadening. The dynamic range contribution, $8D^{-2}f_r^{-1}$, is -148 dBc/Hz at 12 bits and -124 dBc/Hz at 8 bits [16]. Therefore, depending on the system, either laser RIN or dynamic range can dominate Eq. (3). As a useful benchmark, the SNR is $1/\sigma_H \sim 100T^{1/2}$ for $M = 100,000$ resolved elements and a single detector with no filtering at RIN = -145 dBc/Hz.

#123518 - $15.00 USD Received 29 Jan 2010; revised 12 Mar 2010; accepted 15 Mar 2010; published 31 Mar 2010

In our recent work [7, 8], the SNR was limited by the poor dynamic range of $D \sim 500$ at the center of the spectrum and by detector noise at the edges. For the corresponding value of $8D^{-2} f_r^{-1} = $-125 dBc/Hz and the experimental parameters $F \sim 45$ and $\varepsilon = 2$, Eq. (3) yields $M/\sigma_H = 6.7\times10^6$ Hz$^{1/2}$. At the measured M = 41000, $\sigma_H = 4\times10^{-4}$ and T = 2700 sec the measured quality factor was $M/\sigma_H = 2\times10^6$ Hz$^{1/2}$, or ~3 times worse than the calculated value, which is attributed mainly to the rolloff in the SNR on the spectral edges due to reduced comb power (the peak SNR was ~2× better) and to unequal source and LO powers.

We can also compare Eq. (3) to several other demonstrations of fiber-based dual-comb spectroscopy [4, 5]. In the initial cavity-enhancement demonstration of Ref. [5], there were M = 1500 resolved elements. Including a reference scan, the peak SNR $= 100/\sqrt{2}$ and the acquisition time $T = 2\Delta f_r^{-1} \sim 4$ ms. (In [5] the quoted acquisition period is the apodization window, but in Eq. (2) it is the time required for a full scan or Δf_r^{-1}). With these values, the experimental quality factor was $M/\sigma_H = 1.7\times10^6$ Hz$^{1/2}$. In Ref. [4], both sources passed through the sample but the SNR should still apply to within a factor of two. We estimate $M \approx 3100$, $\varepsilon = 115$, an SNR of $\sqrt{2}\times100$ for magnitude, and an acquisition time of $T = 2$ s, to calculate $M/\sigma_H \approx 0.25\times10^6$ Hz$^{1/2}$ (with higher values possible for Δf_r closer to the Nyquist limit).

In general for a single detector, these results, as well as Eq. (3) and Fig. 2, point to a quality factor of $M/\sigma_H < 10^7$ Hz$^{1/2}$ for coherent dual comb spectrometry, at least with fiber-based combs; solid-state combs have lower RIN and could reach higher quality factors.

2.3 Sensitivity to a trace gas

The reconstructed response provides high-frequency resolution and accuracy for characterizing a sample and therefore comes with the potential to detect a particular gas in the presence of large background clutter. The best possible sensitivity (with no background clutter) can be calculated based on Eq. (2). To compare with laser spectrometers, it is useful to express the sensitivity in terms of the minimum absorption sensitivity at a discrete line $(\alpha_0 L)_{\min}$. One might simply equate this to the uncertainty in spectral intensity, $2\sigma_H$. However, the actual sensitivity is considerably better because there are many measured points across a single absorption line and many absorption lines. We derive

$$(\alpha_0 L)_{\min}^{effective} = 2\sigma_H \times \sqrt{\frac{4\nu_{res}}{\pi \sum_j \Delta\nu_{Lor,j} \left(\alpha_j/\alpha_0\right)^2}}, \qquad (4)$$

where the sum is over the different rovibrational lines, each with Lorentzian FWHM $\Delta\nu_{Lor,j}$ and peak absorption α_j. The square root term represents the enhancement over the sensitivity calculated at a single frequency element. For the mock signal of Fig 1, the sum is over 20 equally strong lines with widths ~20×ν_{res}, yielding an enhancement of ~20. More realistically, for example, for the HCN data of Refs. [6-8], the enhancement factor relative to the strongest line is ~11 for ν_{res}=200 MHz. Eq. (4) also assumes the gas response is known. While this enhancement helps, the overall sensitivity is low by the standards of laser spectrometers. As with conventional FTS, this lower sensitivity is a tradeoff with the fact one has access to broadband spectrum.

2.4 Multiplicative noise from residual phase noise between the combs

An important noise contribution in any Fourier spectroscopy is multiplicative noise. It can occur here due to relative amplitude noise, timing jitter or phase noise between the two comb sources. (Shot noise is technically multiplicative but treated as additive here for reasons explained in Section 3.2.) We assume most of the timing and phase noise between the combs

#123518 - $15.00 USD Received 29 Jan 2010; revised 12 Mar 2010; accepted 15 Mar 2010; published 31 Mar 2010

is suppressed either through active phase-locking or monitoring approaches [4, 6-8]. (It would be possible to suppress pulse-to-pulse amplitude noise in this way as well, in principle.) Nevertheless, there will remain residual noise between the combs and it is useful to calculate the effect of this noise on the measured sample response. Carrier phase noise is particularly troublesome even for highly stabilized combs [20], so we concentrate on carrier phase noise rather than timing jitter. We can divide the phase noise into slow and fast components. Phase noise slow compared to the interferogram update rate Δf_r^{-1} will cause a reduction in the summed interferogram signal of $\left(1-\sigma_{\varphi,slow}^2/2\right)$ where $\sigma_{\varphi,slow}^2$ is the (slow) component of the phase variation. For $\sigma_{\varphi,slow}=0.4$ rad, the net effect is a negligible reduction of 8 % [19]. For time scales where $\sigma_{\varphi,slow}>1$ rad, phase correction should be applied in the usual way [8, 16]. With these considerations, slow phase noise is not generally a problem.

Residual fast phase noise that occurs over the timescale of the interferogram (and particularly over the centerburst) cannot be similarly removed. Assuming the noise is small (< 1 radian), it adds a multiplicative noise term that will average down with the square root of the number of interferograms, but can still easily exceed the additive white noise. For example, a 0.1 radian variation leads to ~ 10 % noise over the centerburst, which will completely mask any weak underlying signal. To retain sensitivity in the time domain to the sample response (i.e., FID signal for a trace gas), the centerburst duration ($\sim 1/\Delta\nu_A$) must be shorter than the sample coherence time (~inverse width of the spectral features). In the frequency domain, this multiplicative noise results in phase and amplitude noise with a correlation width equal to the spectral width of the signal in a given sub-band , e.g., $\Delta\nu_A$ yielding a slow baseline wander. To retain sensitivity in the frequency domain to a sample response, the correlation width $\Delta\nu_A$ must be larger than the width of the spectral features (exactly the same condition as in the time domain). The slow wander can be removed by a simple polynomial fit [6-8]. Assuming white carrier phase noise with pulse-to-pulse variance of $\sigma_{\varphi,fast}^2$ and a spacing between filter centers equal to the FWHM, the noise on the magnitude or phase is approximately

$$\sigma_{H,mult} \sim 3\sqrt{\frac{\Delta\nu}{TN_d f_r}}\sigma_{\varphi,fast}, \tag{5}$$

with a Gaussian correlation width equal to the spectral width of the filter or $\Delta\nu_A$. The variables are defined again in Table 1. (See Eq. (30) for a more rigorous expression). This noise can be compared to the white noise of Eq. (2). For N_d = 1 and the values of Fig. 1, $\sigma_{H,mult} \sim 0.1\sigma_{\varphi,fast}\mathrm{Hz}^{-1/2}$. (Note that the shot-noise contribution of the relative phase noise is $\sigma_{\varphi,fast}^{shotnoise} \sim n_c^{-1/2}$, where n_c is the number of photons per pulse. Inserting this into Eq. (5) yields a noise contribution that is $\sim\sqrt{M}$ times smaller than the equivalent shot-noise contribution in Eq. (2).) In general, while this multiplicative noise may be larger than the additive white noise, it is highly correlated across the spectrum; its contribution to the noise across a spectral line of width $\Delta\nu_L$ is only $\sim\left(\Delta\nu_L/\Delta\nu_A\right)\sigma_{H,mult}$. For example, in Refs. [7, 8], $\sigma_{H,mult} \sim 2\sigma_H$ but since $\Delta\nu_A > 100\Delta\nu_L$, the multiplicative noise was negligible. Therefore, through a combination of suppressing residual noise between the combs and the built-in common-mode rejection of Fourier spectroscopy, multiplicative noise can be suppressed in dual comb spectroscopy to a level where it is unimportant. Of course, with greater sequential or parallel filtering, $\Delta\nu_A$ is reduced and there is a corresponding reduction in the effective common mode rejection so that one must be careful to always ensure that this noise contribution remains below Eq. (2).

#123518 - $15.00 USD Received 29 Jan 2010; revised 12 Mar 2010; accepted 15 Mar 2010; published 31 Mar 2010

2.5 Comparison with tunable laser spectrometer & grating spectrometer

It is also useful to compare the SNR of a dual-comb spectrometer to a tunable laser spectrometer (TLS) [17, 18] covering the same bandwidth at the same resolution. We first compare to the dual-comb spectrometer with a single point detector and no filtering ($F = N_d = 1$), ignoring geometry-dependent numerical factors and assuming spectrally flat RIN and comb spectrum. In the detector noise limit, the dual-comb spectrometer is equivalent to a TLS with a power $\sqrt{N_{teeth}} P_{tooth}$ where P_{tooth} is the power per tooth and $N_{teeth} = \Delta\nu / f_r$ is the number of participating comb teeth (equal to M for $\varepsilon = 1$). Of course, the TLS is unlikely to be detector noise limited. In the shot-noise limit, the dual-comb spectrometer is equivalent to a TLS at a power equal to P_{tooth}. In the RIN limit, the dual comb spectrometer is equivalent to a TLS with a RIN that is N_{teeth} greater. The comparison improves if sequential or parallel acquisition is used. For example, in the shot-noise limit the dual-comb spectrometer is equivalent to a TLS with power $N_d P_{tooth}$ and, in the RIN limit, to a TLS with a RIN of $N_{teeth} RIN \Big/ \left(N_d^2 F \right)$.

There are several additional points in favor of dual-comb FTS over TLS. First, the comb spectrum can, in principle, cover spectral regions where a TLS is unavailable. Second, a conventional TLS measures the intensity (amplitude) and does not recover the phase of the signal. It is possible to configure a TLS to measure phase as well as amplitude, but it is difficult to control the phase noise down to the sub-mradian level possible with dual comb spectroscopy. Third, high frequency accuracy and stability is challenging in a fast swept laser system. Fourth, the comb spectrometer can acquire spectra more rapidly than many (but not all) swept lasers and allow for spectral measurements in dynamic systems. This potential for high speed spectral measurements is a strong attribute of dual comb spectroscopy.

2.6 Summary

We derive the basic SNR achievable with a dual comb spectrometer, Eq. (2), considering the effects of additive white noise from detection, shot noise, or RIN due to additive ASE under the assumption of negligible differential chirp, Nyquist filtering, and negligible 1/*f* noise between the combs. This latter assumption requires some combination of a sufficiently high scan rate (Δf_r) and effective phase-locking between the combs through active feedback or monitoring of error signals. We show that under the appropriate conditions, multiplicative noise can be controlled to below the noise level of Eq. (2). We also derive the effective SNR for trace gas detection considering the additive noise of Eq. (2). We allow for the possibility of detecting the entire spectrum at once, sequentially through a tunable filter, or in parallel through a fixed filter and detector array.

The equations can be used to guide the design of dual-comb spectrometers, depending on the contribution of the different noise sources. For example, with appropriate care in treating multiplicative noise, the best SNR is attained through a dual comb spectrometer that uses a detector array. A useful figure of merit, both in terms of the scaling of the SNR and for practical reasons, is the quality factor given by the product of the number of resolved elements and the SNR. For fiber-based systems, it is on the order of 10^6 $Hz^{1/2}$ – 10^7 $Hz^{1/2}$; however, the equations are general and apply as well to future dual comb spectroscopy into the mid- and long-wave infrared. The limit to the sensitivity for measuring a specific gas spectrum will be set by the SNR, the overall path length (which can be quite large for these systems through either cavity enhancement or multipass cells) and the total achievable integration period, which can also be quite large through coherent signal averaging. Although not as sensitive as tunable laser spectrometers, dual-comb spectrometers are promising for broadband detection of multiple gases and for high resolution spectroscopy, due to the excellent frequency resolution and accuracy, the high acquisition speed, and the possibility of accessing spectral regions inaccessible to tunable lasers.

#123518 - $15.00 USD Received 29 Jan 2010; revised 12 Mar 2010; accepted 15 Mar 2010; published 31 Mar 2010

3. Derivations

The organization of this section mirrors that of Section 2, i.e. Section 3.1 derives the basic response of the system, additive noise is considered in 3.2, trace gas sensitivity in 3.3, and multiplicative noise in 3.4. For added insight, the derivation is given in both the time domain, where the data are acquired, and the frequency domain, where they are often used.

As shown in Fig. 1, a single detector will see an "instantaneous" spectral subband of width $\Delta\nu_A = \Delta\nu/(FN_d)$ for an acquisition period $T_A = T/F$. The responses within each spectral sub-band are concatenated in the frequency domain to cover the full source bandwidth, Δν, (and then inverse Fourier transformed to yield the time-domain response). Assuming roughly uniform spectral power, the spectral SNR within a subband $\Delta\nu_A$ is identical to that over the full band $\Delta\nu$, and therefore we need calculate only the SNR in a sub-band. The subscript A is added to the variables in Table 1 to indicate filtered quantities.

3.1 System response

In dual comb spectroscopy, the source and the LO have different pulse repetition periods, T_S and T_L, so that the LO pulses advance through the source pulses by $\Delta T = T_L - T_S$ every LO pulse, yielding a down-conversion factor in time of

$$K \equiv \frac{T_S}{\Delta T} = \frac{T_L}{\Delta T} - 1. \tag{6}$$

that relates laboratory time to effective time. (We take $\Delta T > 0$.) A single pass of the LO pulse through the source pulses generates a single interferogram, which will contain K points and take a time Δf_r^{-1}. Similarly, in the frequency domain, the repetition rates $f_{rS} = T_S^{-1}$ and $f_{rL} = T_L^{-1}$ differ by $\Delta f_r = f_{rS} - f_{rL}$ so that their heterodyne signal is an rf comb with repetition rate Δf_r yielding a down-conversion factor in frequency of [1-8, 13],

$$K \equiv \frac{f_{rL}}{\Delta f_r} = \frac{f_{rS}}{\Delta f_r} - 1. \tag{7}$$

As noted in previous work [19], to achieve fully synchronous sampling, we would like each time-domain interferogram to be identical so that we can simply add them. In the frequency domain, the rf frequency comb then falls exactly on the measured frequency grid, which is not necessary [4] but does simplify the math. To achieve this, we assume [19]:

(1) K is an integer. This condition ensures that the overlap of the K_{th} LO pulse with $(K+1)_{th}$ source pulse has exactly the same time offset as the overlap of the 0th LO and source pulse.

(2) $(K+1)\Delta\theta_{ceo,S} = K\Delta\theta_{ceo,L} + 2\pi q$, where $\Delta\theta_{ceo,S(L)}$ is the carrier-envelope offset (ceo) phase shift per pulse [24, 25] and q is an integer. This insures the relative phase of the K_{th} LO pulse and $(K+1)_{th}$ source pulse is exactly the same as the 0th LO and source pulse. An equivalent condition is that a regular series of comb teeth, $\nu_{0n} = \nu_0 + nKf_{rL}$ sit at identical frequencies for both source and LO combs. For simplicity, we select ν_0 to correspond to the particular "shared" comb tooth, ν_{0n}, closest to the carrier frequency of the filtered light. As the filter is tuned, or for different point detectors, or if a comb offset frequency is shifted (in increments of Δf_r), part of the bookkeeping is to track jumps in ν_0.

(3) The entire instantaneous bandwidth $\Delta\nu_A$ falls between ν_0 and $\nu_0 \pm Kf_{rS}/2$, i.e., $0 < |\nu - \nu_0| < Kf_{rS}/2$. This condition insure there are no rf beats that fall at zero or Nyquist and avoids aliasing effects. Clearly, in an experiment, it is necessary to first shift ν_0 if a portion of the optical spectrum covering a shared tooth, or equidistant between two shared teeth, is to be measured (see Fig. 4).

#123518 - $15.00 USD Received 29 Jan 2010; revised 12 Mar 2010; accepted 15 Mar 2010; published 31 Mar 2010

(4) All spectral filtering is Gaussian with FWHM $\Delta\nu_A$ and a spacing between filtered sub-bands equal to the FWHM. (The formulae then apply to $N_d = F = 1$ for a Gaussian source.)

Figure 4 clarifies the different frequencies involved.

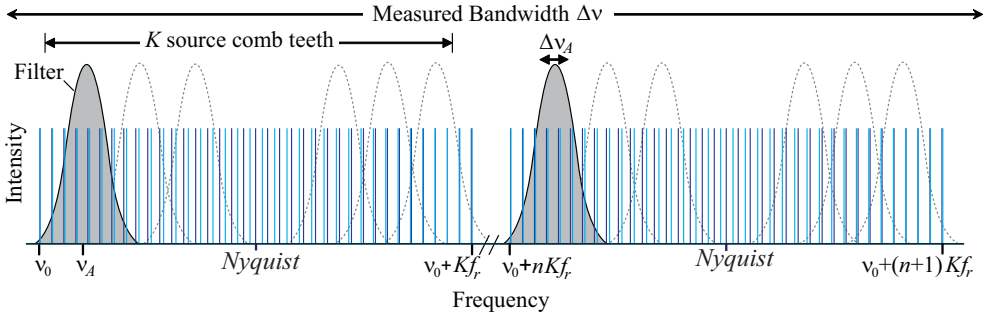

Fig. 4. Schematic of the different optical frequencies involved in the calculation. The light blue (dark blue) lines are the source (LO) comb lines. Their repetition-rate difference is Δf_r. The entire measured bandwidth is $\Delta\nu$, but for any given interferogram, the bandwidth is filtered to $\Delta\nu_A$ either sequentially by tuning the filter across the spectrum or in parallel with a fixed filter bank to multiple detectors (or a combination of the two.) Note the "dead zones" where the rf beat notes are at either zero or Nyquist frequency; at these filter locations an overall frequency shift is applied to one source [7, 8].

Under assumptions 1 and 2 above, the source and LO electric fields are

$$E_S(t) = e^{i\varphi_S} e^{-i2\pi\nu_0 t} \sum_n A_S(t - nT_S),\ E_L(t) = e^{i\varphi_S + \Delta\varphi} e^{-i2\pi\nu_0 t} \sum_m A_L(t - mT_L), \tag{8}$$

where n and m are pulse indices, φ_s and $\Delta\varphi$ are phase factors, ν_0 is the common shared comb tooth, and $A_{S(L)}$ are electric field envelopes. These equations describe two combs with frequencies $\nu_n = \nu_0 \pm nf_{rS}$ and $\nu_m = \nu_0 \pm mf_{rL}$ where n, m are integers. We assume the source and LO pass through the same spectral filter, so that A_L and A_S have identical carrier frequencies, $\nu_A - \nu_0$, and bandwidths, $\Delta\nu_A$. As stated earlier, we assume negligible differential chirp.

The heterodyne portion of the detected voltage is

$$V'(t) = aR(t) \otimes E_L^*(t) E_S(t), \tag{9}$$

where $R(t)$ is the filtering from both hardware and software and a converts from squared electric field to measured photocounts. The voltage is digitized synchronously with the LO comb at a series of times, kT_L, where k is an integer. Substituting (8) into (9) yields $V_k' = V'(t = kT_L) = a\int e^{-i\Delta\varphi} \sum_{n,m} R(\tau') A_L^*((k-m)T_L - \tau') A_S(kT_L - nT_S - \tau')\, d\tau'$.

Rewriting this in terms of the effective time $t_{eff} = k\Delta T$, noting $T_L = T_S + \Delta T$, and with the change of variables $r \equiv n - m$, $p \equiv k - m$, $\tau = \tau' - kT_L + pT_S$, after some rearranging,

$$V'(t_{eff}) = e^{-i\Delta\varphi} \sum_{r=0}^{r=T/T_{frame}} V(t_{eff} - rT_S), \tag{10}$$

where the individual terms (interferograms) are

$$V(t) = \int S(t') A_S(t - t')\, dt' \equiv S(t) \otimes A_s(t), \tag{11}$$

with a sampling function $S(t) = a\sum_p R(pT_S + t) A_L^*(p\Delta T - t)$.

Eq. (10) simply describes a series of concatenated interferograms. If Fourier transformed, one finds the rf comb of Ref. [6]. However, it is simpler to just add the individual

#123518 - $15.00 USD Received 29 Jan 2010; revised 12 Mar 2010; accepted 15 Mar 2010; published 31 Mar 2010

interferograms, and just as effective in terms of noise suppression. With the assumption of synchronous sampling, there is no phase shift between interferograms, and the grid of time points, $t_{eff} = k\Delta T$ is aligned with the effective time offset T_S, so that no interpolation is required in calculating the average interferogram, $\langle V(t_{eff})\rangle$. Henceforth, we drop the brackets and let $t_{eff} \to t$. Under assumption 3 above, ΔT is sufficiently short that $p\Delta T$ is effectively a continuous variable ($p\Delta T \to \tau$), and the sum for $S(t)$ can be rewritten as $S(t) \approx a\Delta T^{-1}\int R(K\tau + t)A_L^*(\tau - t)d\tau$ with Eq. (6). With a change of variables,

$$S(t) = a\Delta T^{-1}\, R[(K+1)t] \otimes A_L^*\left[-\left(\frac{K+1}{K}\right)t\right]. \tag{12}$$

In the limit $K >> 1$ and a broad detection bandwidth, $S(t) \approx A_L^*(-t)$, as expected.

From a frequency-domain point of view, Eq. (8) in the limit of a long pulse train is also

$$\begin{aligned} E_S(t) &= e^{i\varphi_S} e^{-i2\pi\nu_0 t}\sum_q \tilde{A}_S(qf_{rS})e^{-i2\pi qf_{rS}t} \\ E_L(t) &= e^{i\varphi_S+\Delta\varphi} e^{-i2\pi\nu_0 t}\sum_p \tilde{A}_L(pf_{rL})e^{-i2\pi pf_{rL}t}, \end{aligned} \tag{13}$$

where q, p are integers. Substitution into Eq. (9) gives $V(t) = e^{i\Delta\varphi}\sum_{p,q}\int d\tau df\, \tilde{R}(f)e^{-i2\pi f\tau}\tilde{A}_L^*(pf_{rL})\tilde{A}_S(qf_{rS})e^{i2\pi pf_{rL}(t-\tau)}e^{-i2\pi qf_{rS}(t-\tau)}$. Letting $p = w+q$, and carrying out the integrations,

$$V'(t) = e^{-i\Delta\varphi}a\sum_{w,q}\tilde{R}(q\Delta f_r - wf_{rL})\tilde{A}_L^*(qf_{rL} + wf_{rL})\tilde{A}_S(qf_{rS})e^{-i2\pi q\Delta f_r t}e^{i2\pi wf_{rL}t}. \tag{14}$$

Only the $w = 0$ term survives, and there is a finite range of q, giving

$$V'(t) = e^{-i\Delta\varphi}a\sum_{q=q_{\min}}^{q=q_{\max}}\tilde{R}(q\Delta f_r)\tilde{A}_L^*(qf_{rL})\tilde{A}_S(qf_{rS})e^{-i2\pi q\Delta f_r t}, \tag{15}$$

with the Fourier transform

$$\tilde{V}'(f) = e^{-i\Delta\varphi}a\sum_{q=q_{\min}}^{q=q_{\max}}\tilde{R}(q\Delta f_r)\tilde{A}_L^*(qf_{rL})\tilde{A}_S(qf_{rS})\delta(f - q\Delta f_r), \tag{16}$$

or the standard "multi-heterodyne" result modified to account for the frequency response of the detector: an rf comb where each tooth at $q\Delta f_r$ is the beat between the neighboring q^{th} comb lines [1, 2, 6]. We rewrite this in terms of the optical frequencies $\nu = (K+1)f$ as $\tilde{V}'(\nu) = e^{-i\Delta\varphi}a(K+1)^{-1}\tilde{R}(\nu/(K+1))\tilde{A}_L^*(\nu K/(K+1))\tilde{A}_S(\nu)\sum_q\delta(\nu - qf_{rS})$. We observe for only a finite time so the delta function should be a sinc function; however, we sample on the grid of $\nu = qf_{rS}$, and the values are unchanged and

$$\tilde{V}(\nu) = e^{-i\Delta\varphi}\tilde{S}(\nu)\tilde{A}_S(\nu), \tag{17}$$

where

$$\tilde{S}(\nu) = \frac{a}{K+1}\tilde{R}\left(\frac{\nu}{K+1}\right)\tilde{A}_L^*\left(\frac{K}{K+1}\nu\right), \tag{18}$$

or the transform of Eq. (12). Reinstating ν_0, so that $A_{S(L)} \to E_{S(L)}$, Fourier transforming, adding the effect of the sample response, and a noise term, gives

#123518 - $15.00 USD Received 29 Jan 2010; revised 12 Mar 2010; accepted 15 Mar 2010; published 31 Mar 2010

$$V(t) = S(t) \otimes E_S(t) \otimes H(t) + \frac{n(t)}{\sqrt{T_A \Delta f_r}}, \tag{19}$$

evaluated at K time points separated by ΔT and covering a time window T_S, where $n(t)$ is the noise in a single interferogram, which is reduced by the square root of the number of averaged interferograms equal to $T_A \Delta f_r$. The interferogram has the appearance shown in Fig. 1 of a centerburst, oscillating at a frequency $|\nu_A - \nu_0|$ and with a width $\sim \Delta \nu_A^{-1}$. If $n(t)$ has a standard deviation σ_t, the peak time-domain signal-to-noise ratio is

$$(S/N)_t = \sqrt{T_A \Delta f_r}\, \frac{V(0)}{\sigma_t}. \tag{20}$$

In the frequency (spectral) domain, the Fourier transform of (19) yields

$$\tilde{V}(\nu) = \tilde{S}(\nu) \tilde{E}_S(\nu) \tilde{H}(\nu) + \frac{\tilde{n}(\nu)}{\sqrt{T_A \Delta f_r}}, \tag{21}$$

evaluated at (K/2+1) frequency points separated by f_{rS} and covering a bandwidth $(2\Delta T)^{-1}$ with an optical frequency offset ν_0. The SNR in either quadrature is

$$(S/N)_\nu = \sqrt{T_A \Delta f_r}\, \frac{\tilde{V}(\nu)}{\sigma_\nu}, \tag{22}$$

where the noise term $\tilde{n}(\nu)$ has equal real and imaginary standard deviations, σ_ν.

This SNR applies to both the reference and signal of Eq. (1). Therefore, the noise on the normalized transmittance, or sample response is

$$\sigma_H = \frac{2}{(S/N)_\nu}, \tag{23}$$

where the numerator includes one factor of √2 from comparing reference and signal and one factor of √2 from the fact that equal periods must be spent measuring reference and signal. At this point, the detector response, $R(\nu)$ drops out. We will assume a bandwidth matched to Nyquist (thus avoiding aliased noise) but otherwise ignore $R(\nu)$ below.

3.2 Contributions of additive white noise sources

We now derive Eq. (2). The additive, white, Gaussian noise from detector noise, shot-noise and laser RIN to each interferogram has standard deviation

$$\sigma_t = \sqrt{\sigma_d^2 + \eta n_S + \eta n_{LO} + (RIN_S)(f_r/2)\eta^2 n_L^2 + (RIN_L)(f_r/2)\eta^2 n_S^2}. \tag{24}$$

The first term is the detector and digitizer noise contribution, σ_d (in units of photon counts). The second and third term are shot noise, where $n_{S(LO)}$ is the number of photons per source (LO) pulse within the filtered band $\Delta \nu_A$. The shot-noise term is technically multiplicative, as it varies over the centerburst, but if the centerburst is short compared to the interferogram, we ignore this variation. The last two terms arise from the excess RIN of the lasers, which we assume here arises from an additive ASE field. This RIN is white so that variation in photons per pulse δn_S is $(\delta n_S / n_S)^2 = RIN_S(f_r/2)$ since the RIN is single-sided. With balanced detection, this RIN from each individual laser is cancelled. However, the noise from the LO pulses beating against the source ASE component, and vice versa, is not cancelled and leads

#123518 - $15.00 USD Received 29 Jan 2010; revised 12 Mar 2010; accepted 15 Mar 2010; published 31 Mar 2010

to the 4th and 5th terms in Eq. (24). Without balanced detection, the RIN contribution is twice as big. The peak signal for the interferogram is $V(0) = 2\eta\sqrt{n_S n_{LO}} = 2\eta\sqrt{\gamma} n_S$ and Eq. (20) becomes,

$$(S/N)_t = \sqrt{T_A \Delta f_r}\, \frac{2\eta n_S}{\sqrt{\gamma^{-1}\sigma_d^2 + 2c_\gamma \eta n_S + c_{\gamma^2} b(RIN) f_r \eta^2 n_S^2 + 4D^{-2}\eta^2 n_S^2}}, \tag{25}$$

where $c_\gamma = (1+\gamma)/(2\gamma)$, $c_{\gamma^2} = (1+\gamma^2)/(2\gamma)$ for $RIN_L = RIN_S = RIN$ and we introduce the parameter b =1(2) for balanced (unbalanced) optical detection. The last term in the denominator is added to include experimental dynamic range limitations in the detection that clamp the SNR of a single interferogram to *D*. The fraction in brackets is the SNR of a single interferogram; for $\gamma = 1$; it equals $\sqrt{2\eta n_S}$ in the shot-noise limit and D in the dynamic range limit, which can be set by the photodetection, amplification or digitizer.

Under the assumption of white noise, the frequency domain is $(S/N)_\nu = \left(\sqrt{2/K}\, |\tilde{V}(\nu)| / \langle |\tilde{V}(\nu)| \rangle\right) \times (S/N)_t$, where the brackets indicates the mean value across the measured spectrum [16]. An average of the numerator over the central FWHM of the gaussian signal spectrum, denoted $\langle\ \rangle_{\Delta\nu_A}$, gives the ratio $\langle |\tilde{V}(\nu)| \rangle_{\Delta\nu_A} / \langle |\tilde{V}(\nu)| \rangle = K f_r \mathrm{erf}\left(\sqrt{\ln(2)}\right)/(2\Delta\nu_A) \sim 0.4 K f_r/\Delta\nu_A$ for $\Delta\nu_A << (2\Delta T)^{-1}$ (which is true to avoid aliasing). With $P_{cA} \equiv h\nu f_r n_s$, in the frequency-domain Eq. (25) becomes,

$$(S/N)_\nu = 0.8\frac{\sqrt{T_A}}{M_A}\, \frac{2P_{cA}}{\sqrt{\gamma^{-1} NEP^2 + 4c_\gamma \eta^{-1} h\nu P_{cA} + 2bc_{\gamma^2}(RIN) P_{cA}^2 + 8D^{-2} f_r^{-1} P_{cA}^2}}, \tag{26}$$

where we use $f_{rS} \approx f_{rL} \approx f_r$, $M_A = \Delta\nu_A / f_r$, and the equality $\sigma_d \eta^{-1} h\nu = NEP/\sqrt{2 f_r}$. Assuming this same SNR is achieved across the full spectrum (i.e., the RIN and power are spectrally flat), and accounting for spectral reconstruction we substitute $T_A = T/F$, $M = M_A(\Delta\nu/\Delta\nu_A)$, $P_c = P_{c,A}(\Delta\nu/\Delta\nu_A)$ and $\Delta\nu_A = \Delta\nu/(FN_d)$ into Eq. (26), and the result into Eq. (23),

$$\sigma_H = \frac{M}{\sqrt{T}} \left\{ \frac{1}{0.8} \sqrt{\left(\frac{NEP}{P_c}\right)^2 \gamma^{-1} F + c_\gamma \left(\frac{4h\nu}{\eta P_c}\right) \frac{1}{N_d} + 2bc_{\gamma^2} \frac{RIN}{FN_d^2} + \frac{8}{D^2 f_r F N_d^2}} \right\}. \tag{27}$$

This uncertainty can be improved by smoothing (i.e., apodizing in the time domain) to a resolution of ν_{res}. In that case, we redefine $M = \Delta\nu/\nu_{res}$ to retain its definition as the number of resolved elements and multiply by $\sqrt{\varepsilon} = \sqrt{\nu_{res}/f_r}$ to finally reach (2).

It is easier to derive the same expression (27) entirely in the frequency domain. For simplicity, we take $\gamma = 1$ so that the power per tooth, P_{tooth}, is the same for the source and LO combs. The rms signal amplitude between two teeth is $\sqrt{2}\eta P_{tooth}$ at an rf frequency corresponding to their optical frequency difference. The white noise power is $\left[\eta^2 NEP^2 + 4\eta h\nu P_{cA} + 2b\eta^2 P_{cA}^2 (RIN)\right] B$, where the first term is detector noise, the second term is the shot noise associated with the two sources, and the third term is the RIN of the two sources. Note that both the shot noise and RIN are given by the total comb power P_{cA}. The

#123518 - $15.00 USD Received 29 Jan 2010; revised 12 Mar 2010; accepted 15 Mar 2010; published 31 Mar 2010

effective bandwidth is $B = 1/(2T_A)$. This random noise power contributes equally to the amplitude and phase noise, and

$$(S/N)_\nu = \frac{2\sqrt{T_A}P_{tooth}}{\sqrt{NEP^2 + 4\eta^{-1}h\nu P_{cA} + 2bP_{cA}^2 RIN}}. \quad (28)$$

Averaged across the FWHM of an assumed Gaussian spectrum, the comb tooth power is $P_{tooth} = 0.8P_{cA}/M_A$ and Eq. (28) is exactly Eq. (26) after reinstating γ and introducing *D*.

3.3 Sensitivity to a known gas

A weakly absorbing gas with density ρ and sample length L will have a time-domain response equal to $H(t) = \mathrm{sinc}(\pi t\Delta\nu) \otimes [\delta(t) + \rho LF(t)]$, where the sinc term reflects the instrument response over the bandwidth $\Delta\nu$ and the term in square brackets is the sample response characterized by the function $F(t)$. We use a standard matched filter approach by defining a cutoff time t_0. We mask out points earlier than t_0 to avoid the multiplicative noise across the centerburst. The uncertainty in the column density, ρL, is $\sigma_{\rho L} = \sigma_{t,R} \Big/ \sqrt{\sum_{t_i>t_0}^{t_i=T_S} F^2(t_i)} = \sigma_H \sqrt{2\nu_{res}} \Big/ \sqrt{\int_{t_0}^{T_S} \left|F^2(t)\right|^2}$, where $\sigma_{t,R} = \sigma_H/\sqrt{M}$ is the standard deviation of the spectrally reconstructed time-domain interferogram (See Fig. 1). For a Voigt profile, a single absorption line at ν_j with integrated line strength S_j has a time-dependent response $F_j(t) = S_j\theta(t)e^{-2\pi i\nu_j t}e^{-\pi^2\Delta\nu_D^2 t^2/(4\ln 2) - \pi\Delta\nu_{Lor,j}t}$, where $\Delta\nu_D$ is the FWHM Doppler width, $\Delta\nu_{Lor}$ is the FWHM Lorentzian width and $\theta(t)$ is the Heavyside step function. (This time-dependent signal is exactly the free induction decay). We will assume a collisionally broadened line ($\Delta\nu_{Lor} > \Delta\nu_D$). If $t_0 << \Delta\nu_{Lor,j}^{-1} << f_{rS}^{-1}$, the limits on the integral are 0 and ∞ and $\sigma_{\rho L} = \sigma_H \sqrt{2\nu_{res}} \Big/ \sqrt{\sum_j S_j^2 (2\pi\Delta\nu_{Lor,j})^{-1}}$, where the sum is over all observed lines. The peak absorption of a given line is $\alpha_j = 2\rho S_j/(\pi\Delta\nu_{Lor,j})$ for a Lorentzian. To rewrite this in a more conventional form, we let $\sigma_{\rho L} = (\rho L)_{\min}$, the minimum detectable column density, and then scale it by a particular reference line (denoted $j = 0$), to find the effective minimum absorption, normalized to a reference line, $(\alpha_0 L)_{\min}^{effective} \equiv 2S_0(\pi\Delta\nu_{Lor})^{-1}(\rho L)_{\min}$, or Eq. (4).

3.4 Multiplicative noise from residual phase noise between combs

The combs will exhibit residual amplitude, timing and phase jitter between pulses since no effort to remove the residual noise will be perfect. The carrier phase noise is typically dominant because it is the most challenging to control and, particularly outside the locking or monitoring bandwidth, the combs will have some residual high-frequency phase variations [20]. As a result, the first term of Eq. (19) is modified to $V(t) \to e^{i\delta\varphi(Kt)}V(t)$, where the exponent describes the relative carrier phase jitter as a function of laboratory time. The fast phase variations are particularly problematic (see Section 2.5). If small (< 1 rad), they add a multiplicative noise $n(t) = iV(t)\delta\varphi(t)$ to Eq. (19). From a generalized Eq. (22) and (23),

$$\sigma_{H,mult}^2(\nu,\nu') = \left(\frac{4}{T_A\Delta f_r}\right)\frac{\left\langle\tilde{n}(\nu)\tilde{n}^*(\nu')\right\rangle}{\tilde{V}(\nu)\tilde{V}^*(\nu')} \quad (29)$$

#123518 - $15.00 USD Received 29 Jan 2010; revised 12 Mar 2010; accepted 15 Mar 2010; published 31 Mar 2010

is the covariance with $\tilde{n}(\nu)=\tilde{\varphi}\left((\nu-\nu_0)/K\right)\otimes i\tilde{V}(\nu)$. Assuming a pulse-to-pulse phase variance of $\sigma^2_{\varphi,fast}$, $\left\langle\tilde{\varphi}(f)\tilde{\varphi}^*(f')\right\rangle=\sigma^2_{\varphi,fast}f_r^{-1}\delta(f-f')$ and a Gaussian filter profile, $V(\nu)=\exp\left[-4\ln(2)(\nu-\nu_A)^2/\Delta\nu_A^2\right]$,

$$\sigma_{H,mult}(\nu,\nu')\approx\left(\frac{2\pi}{\ln(2)}\right)^{1/4}\sqrt{\frac{\Delta\nu_A}{T_A f_r^2}}\sigma_{\varphi,fast}e^{4\ln(2)(\bar{\nu}-\nu_A)^2/\Delta\nu_A^2}\quad,\quad(30)$$

where $\bar{\nu}=(\nu+\nu')/2$. As expected, the noise increases exponentially in the wings of the spectrum, because the white phase noise will lead to broadband noise while the signal is falling exponentially. At the center, $\nu=\nu'=\nu_A$, the noise is just the prefactor to the exponent in Eq. (30). We restrict the data to the FWHM or $\nu_A-\Delta\nu_A/2<\nu<\nu_A+\Delta\nu_A/2$. The correlated noise is removed through phase correction; the remaining uncorrelated noise is $\sqrt{3}$ times the prefactor in (30). Substituting, $T=FT_A$ and $\Delta\nu=N_dF\Delta\nu_A$, we reach Eq. (5). Similar derivations can be made of relative jitter in effective time, δt, or relative fractional amplitude noise, δa, with the substitution of $n(t)=(\delta t)dV(t)/dt$ or $n(t)=(\delta a)V(t)$ respectively.

Acknowledgements

This research was supported by the Department of Homeland Security and by the National Institute of Standards and Technology. The authors thank Fabrizio Giorgetta, Alex Zolot and anonymous reviewer for useful comments.

#123518 - $15.00 USD Received 29 Jan 2010; revised 12 Mar 2010; accepted 15 Mar 2010; published 31 Mar 2010